Title

Stimulation of soil respiration by elevated CO2 is enhanced under nitrogen limitation in a decade-long grassland study

Journal

Proceedings of the National Academy of Sciences of the United States of America, 117(52)

ISSN

0027-8424

Authors

Gao, Qun

Wang, Gangsheng

Xue, Kai

et al.

Publication Date

2020-12-29

DOI

10.1073/pnas.2002780117

Peer reviewed

Stimulation of soil respiration by elevated CO_2 is enhanced under nitrogen limitation in a decade-long grassland study

Qun Gao[a#], Gangsheng Wang[b#], Kai Xue[b,c], Yunfeng Yang[a*], Jianping Xie[b,d], Hao Yu[b,e,f], Shijie Bai[b,g], Feifei Liu[b,h], Zhili He[b,i], Daliang Ning[b], Sarah E Hobbie[j], Peter B Reich[k,l] and Jizhong Zhou[a,b,m*]

[a]State Key Joint Laboratory of Environment Simulation and Pollution Control, School of Environment, Tsinghua University, Beijing 100084, China;

[b]Institute for Environmental Genomics, Department of Microbiology and Plant Biology, and School of Civil Engineering and Environmental Sciences, University of Oklahoma, Norman, OK 73019, USA;

[c]College of Resources and Environment, University of Chinese Academy of Sciences, Beijing 100190, China;

[d]School of Minerals Processing and Bioengineering, Central South University, Changsha, Hunan 410083, China

[e]College of Environmental Science and Engineering, Liaoning Technical University, Fuxin, Liaoning 123000, China;

[f]Key Laboratory of Environmental Biotechnology, Research Center for Eco-Environmental Sciences, Chinese Academy of Sciences, Beijing 100085, China;

[g]Deep Sea Science Division, Institute of Deep Sea Science and Engineering, Chinese Academy of Sciences, Sanya, Hainan 572000, China

[h]Guangdong Provincial Key Laboratory of Microbial Culture Collection and Application, Guangdong Institute of Microbiology, Guangdong Academy of Sciences, Guangzhou 510070, China;

[i]Environmental Microbiomics Research Center, School of Environmental Science and Engineering, Sun Yat-Sen University, Guangzhou 510006, China

[j]Department of Ecology, Evolution and Behavior, University of Minnesota, St Paul, MN 55108, USA;

[k]Department of Forest Resources, University of Minnesota, St Paul, MN 55108, USA;

[l]Hawkesbury Institute for the Environment, Western Sydney University, Penrith, New South Wales 2753, Australia;

[m]Earth and Environmental Sciences, Lawrence Berkeley National Laboratory, Berkeley, CA 94720, USA;

*Corresponding authors: Yunfeng Yang; E-mail: yangyf@tsinghua.edu.cn; Jizhong Zhou; E-mail: jzhou@ou.edu

[#]The authors contribute equally to this manuscript

Classification

Biological Sciences/Ecology

Keywords

elevated CO_2; nitrogen deposition; soil respiration; metagenomics; Earth ecosystem model

Author Contributions

All authors contributed intellectual input and assistance to this study and manuscript preparation. The original concept and experimental strategy were developed by J.Z., P.R., and S.H.. Field experiments are maintained by P.R. and S.H.. Sampling collections, DNA preparation, and GeoChip hybridization analysis were carried out by K.X., F.L., and Q.G.. Soil chemical analysis was carried out by K.X. and F.L. Carbon-Nitrogen coupled MEND model was developed by G.W.. Modeling was done by G.W. and Q.G. Various statistical analyses were carried out by Q.G., and G.W. All data analyses and integration were guided by J.Z and Y.Y.. The paper was written by Q.G., Y.Y., and J.Z., with help from G.W., P.R., and S.H. Considering their contributions in terms of data collection, analyses, and model-data integration, Q.G. and G.W. are listed as co-first authors.

This PDF file includes:

Main Text

Figures 1 to 3

Table 1

Abstract

Whether and how CO_2 and nitrogen (N) availability interact to influence carbon (C) cycling processes such as soil respiration remains a question of considerable uncertainty in projecting future C-climate feedbacks, which are strongly influenced by multiple global change drivers, including elevated atmospheric CO_2 concentrations (eCO_2), and increased N deposition. However, because decades of research on the responses of ecosystems to eCO_2 and N enrichment have been done largely independently, their interactive effects on soil respiratory CO_2 efflux remain unresolved. Here, we show that in a multifactor free-air CO_2 enrichment experiment, BioCON (Biodiversity, CO_2 and N deposition) in Minnesota, USA, the positive response of soil respiration to eCO_2 gradually strengthened at ambient (low) N supply, but not enriched (high) N supply for the 12-year experimental period from 1998 to 2009. In contrast to earlier years, eCO_2 stimulated soil respiration twice as much at low than at high N supply from 2006 to 2009. In parallel, microbial C degradation genes were significantly boosted by eCO_2 at low but not high N supply. Incorporating those functional genes into a coupled C-N ecosystem model reduced model parameter uncertainty and improved the projections of the effects of different CO_2 and N levels on soil respiration. If our observed results generalize to other ecosystems, they imply widely positive effects of eCO_2 on soil respiration even in infertile systems.

Significance

The magnitude of CO_2 efflux from soils (resulting from autotrophic and heterotrophic respiration) is one of the largest uncertainties in projecting future carbon-climate

feedbacks. Despite research over several decades, the magnitude, direction, and duration of such feedbacks and their underlying microbial mechanisms are poorly understood, especially in the context of potentially interacting global environmental changes. In a decade-long experiment examining the interactive effects of CO_2 and N enrichment, N limitation strengthened the stimulatory effects of eCO_2 on soil respiration, primarily via N mining during the decomposition of more recalcitrant organic compounds. This study also provides a novel strategy for integrating genomics information into ecosystem and Earth system models to improve carbon cycle predictions.

Introduction

Elevation of atmospheric CO_2 concentrations, owing to fossil fuel combustion and land-use changes, represents one of the greatest scientific and political concerns of the 21st century (1). Carbon (C) movement into the atmosphere annually from soils (i.e., soil CO_2 efflux or soil respiration) is much larger than annual C emissions from fossil fuel combustion (2), and thus even small changes in soil respiration could have significant impacts on the pace of change in atmospheric CO_2. Numerous studies have demonstrated that elevated CO_2 (eCO_2) has a direct stimulatory effect on rates of plant photosynthesis (3), and an indirect positive effect on soil respiration, which typically includes autotrophic respiration from plant roots and heterotrophic respiration from microbial decomposition of litter and soil organic matter (SOM). The eCO_2 stimulatory effect on soil respiration is commonly attributed to the following three mutually non-exclusive mechanisms from the actions of plants and microorganisms (4-7): enhanced root respiration associated with greater belowground plant biomass, enhanced microbial

decomposition of fresh C due to greater supply of foliar and root-derived labile soil C, and increased microbial priming of old SOM fueled by this increased supply of labile soil C (4, 5). The stimulation of soil respiration by eCO_2 (7, 8) has the potential to greatly accelerate the future rate of increase in atmospheric CO_2 concentrations unless matched by an offsetting increase in net C uptake.

Human activities have also increased nitrogen (N) deposition to natural ecosystems (9). N enrichment is a growing concern because it disturbs N cycle processes in many ecosystems (9). Various studies have suggested that N addition can either increase (10, 11) or reduce (12-15) soil CO_2 efflux, while other studies have suggested that N addition does not influence soil CO_2 efflux (16, 17), depending on ecosystem type and season of the year.

The stimulation of soil respiration by eCO_2 also could be strongly influenced by variability in ambient soil N availability and the rate of atmospheric N deposition (18). However, studies that have explored the interactive effects of eCO_2 and N on soil respiration are extremely scarce. For instance, an open-top study of young subtropical tree seedlings in contrasting eCO_2 and N treatments in transplanted soil found that response to eCO_2 was enhanced by high levels of N addition (10 g m^{-2} yr^{-1}) in the earliest two years but unaffected by the same N supply in the subsequent year (19, 20). A free-air enrichment study in perennial grasslands also found no interaction between eCO_2 and N addition treatments over the first two years of the study (21). Given that many questions about such potential interactions remain unresolved (22), here we report on 12 years of results in that same grassland study, assessing whether interactions develop, and if so, what underlying mechanisms might drive them.

It is well known that N availability alters many aspects of ecosystems (12, 23, 24) and thus could hypothetically influence responses of soil respiration to eCO_2. Three potentially off-setting and interrelated mechanisms have been proposed. First, N limitation could affect belowground productivity and thus root respiration. For example, if N limitation constrains plant canopy development and the stimulatory effect of eCO_2 on photosynthesis, and thus limits total productivity belowground, root respiration will decline (24). On the other hand, the same N limitation constraint on canopy development combined with stimulatory effects of eCO_2 on photosynthesis could increase plant investment of C in nutrient-absorbing systems (25, 26), favoring C allocation to roots at the expense of aboveground biomass. Such a shift in allocation could increase root respiration (27). Second, changes in root detrital production and exudation of labile C into soils can influence substrate supply that fuels soil microbial activity and heterotrophic respiration. Third, the supply of labile C into soils can influence decomposition of SOM through the priming effect, which would also influence soil heterotrophic respiration (28). Under N limitation, greater photosynthesis caused by eCO_2 could stimulate mining of N from SOM, and thus soil heterotrophic respiration, through enhanced priming mechanisms (29).

Although various studies indicate that N availability plays critical roles in mediating soil respiration (10-17, 23, 30, 31), divergent results are observed: positive (10, 11, 23), neutral (16, 17, 30), or negative (12-15, 30, 31). Thus, the impacts of N availability on the magnitude and duration of the eCO_2 enhancement of soil respiration and its underlying mechanisms remain elusive, particularly under field settings. In addition, recent modeling efforts demonstrated the importance of understanding microbial C

decomposition for more confidently extrapolating soil C cycling processes (32, 33). However, to date, it remains uncertain whether and how microbial processes influence the responses of terrestrial ecosystems to eCO_2 and N deposition, and how best to incorporate information regarding microbial responses to eCO_2 and N into climate-C models for better simulation and prediction (32, 34, 35).

Herein, we report results from a well-replicated long-term (12 years at the time of sampling) CO_2×N experiment, BioCON (24), to elucidate the interactive effects of eCO_2 and N enrichment on soil respiration and their underlying mechanisms. From 1998-2009, we measured soil CO_2 efflux, and other biogeochemical processes on 296 plots containing different numbers (1, 4, 9, or 16 species) and combinations (C_3 and C_4 grasses, forbs, and legumes) of perennial plant species at ambient CO_2 (aCO_2) or eCO_2 (+180 ppm) with either ambient N supply (aN) or enriched N supply (eN, i.e., + 4 g N m^{-2} yr^{-1}). Hereafter, we refer to these four treatment combinations as aCO_2-aN, eCO_2-aN, aCO_2-eN, and eCO_2-eN. The contrasting high versus low levels of N supply in this study was a rough proxy for a part of the worldwide range of N supply rates in soils as well as for times or places with low versus high N deposition (24). Thus, we posit that the results are relevant to understanding the potentially different responses to eCO_2 of both low versus high N fertility soils and contexts with low versus high N deposition. In 2009, we also assessed responses of microbial community functional gene structure to eCO_2 and N enrichment to gain insights into microbial regulation of soil respiration. In addition, we incorporated microbial functional trait information into ecosystem models to explore means of better prediction of C cycling. Our overarching hypothesis is that N limitation would accelerate the stimulatory effects of eCO_2 on soil respiration, primarily via

179 microbial N mining mechanisms. We further explored the possibility that microbial
180 functional trait information would greatly help to constrain the uncertainty of model
181 parameters and hence significantly improve confidence in model simulations and
182 predictions.
183
184 **Results and Discussion**
185 **N modulation of the stimulatory effect of eCO_2 on soil respiration**
186 Soil CO_2 efflux was measured ca. biweekly during the growing season (May to August)
187 from 1998 to 2009. Overall, significantly ($p < 0.01$) higher soil respiration was observed
188 at eCO_2 than aCO_2 at both low and high N supply (Fig. 1a), indicating that eCO_2
189 stimulated soil respiration, consistent with previous reports (6, 7). Along with significant
190 main effects of CO_2, N, and plant species diversity as individual treatments, there were
191 significant CO_2×N ($p = 0.03$; Table 1) and CO_2×N×Year ($p = 0.05$) interactive effects on
192 soil respiration, indicating that the stimulatory effect of eCO_2 on soil respiration was
193 modulated by N supply and that this interaction varied with time. Although the effect of
194 eCO_2 varied with plant diversity ($p = 0.01$ for the CO_2×plant diversity interaction; Table
195 1), the CO_2×N interaction was independent of plant diversity ($p = 0.83$ for the three-way
196 interaction of CO_2×N×plant diversity; Table 1).
197 To better identify the timing of the shift in the responses of soil respiration to eCO_2
198 at contrasting N supplies, four commonly used change-point tests - Pettitt's test, Buishand
199 range test, Buishand U test, and Standard Normal Homogeneity Test (*SI Appendix*, Table
200 S1) - were used. Our results indicated that 2005 was the breakpoint when the N influence
201 on the stimulatory effects of eCO_2 on soil respiration significantly changed (*SI Appendix*,

202 Table S1). Therefore, we have divided the whole experimental period into two phases:
203 Phase I from 1998 to 2005, and Phase II from 2006 to 2009 (see Materials and methods
204 for details). Using this breakpoint, the CO_2×N interactive effects on soil respiration
205 significantly differed between these two phases, as indicated by a significant three-way
206 interaction, CO_2×N×Phase, on soil respiration (p = 0.02; *SI Appendix*, Table S2). In
207 Phase I, eCO_2 significantly (p < 0.01) stimulated mean soil respiration regardless of N
208 level (+22% vs. +24% at low and high N, respectively, Fig. 1b; p = 0.07 for the CO_2×N
209 interaction, *SI Appendix*, Table S3). In contrast, the CO_2×N interaction became
210 significant (p < 0.01; *SI Appendix*, Table S3) in Phase II, and eCO_2 stimulated mean soil
211 respiration by 40% at low N supply, but by only 19% at high N supply (Fig. 1c). These
212 results indicate that long term N limitation strengthened the stimulatory effects of eCO_2
213 on soil respiration as the experiment proceeded.

214 Conceptually, the changing interactive effects of N and eCO_2 on soil respiration
215 between Phase I and Phase II were most likely due to soil processes, plant characteristics,
216 and microbial community structure (21, 34, 36-40). Similar to soil respiration, significant
217 (p < 0.01) CO_2×N×Phase interactions were observed for soil net N mineralization rate
218 and aboveground plant N concentration, but not for other soil and plant variables (*SI*
219 *Appendix*, Table S2), indicating that there were temporal shifts in CO_2×N effects on those
220 two variables. By examining the CO_2×N effect per year from 1998-2009, we found that
221 the CO_2×N effect on soil respiration was significantly correlated with that on soil net N
222 mineralization rate (p = 0.05), aboveground plant N concentration (p = 0.04), and
223 aboveground plant C/N ratio (p = 0.03) (*SI Appendix*, Table S4). Further analysis
224 revealed that eCO_2 had no effect on net N mineralization rate at both N supplies in Phase

I, but significantly increased the mineralization rate at high, but not low N supply, in Phase II (*SI Appendix*, Fig. S1a-b). In addition, aboveground plant N concentration was 8% lower at low than high N supply in Phase I but was 20% lower in Phase II (*SI Appendix*, Fig. S1c-d). These data suggest that soil and plant N availability became more limited at low than high N supply as the time proceeded. The progressive N limitation could lead to less C allocation by plants to grow but more labile C inputs by eCO_2 at low N supply (41), stimulating SOM decomposition and soil respiration. Collectively, the more positive soil respiration response to eCO_2 at lower than higher N supply in Phase II is probably related, at least in part, to the N-mediated phase shift of soil and plant N dynamics in response to eCO_2. Similarly, microbes play important roles in regulating the interactive effects of CO_2 and N on soil respiration, as discussed in the following section.

Roles of microbial processes

The stimulation of soil respiration by eCO_2 might be caused by changes in heterotrophic microbial processes and/or root-associated autotrophic processes (26). However, partitioning soil respiration into autotrophic and heterotrophic respiration is generally difficult (42). Thus, we used root biomass as a proxy to determine whether autotrophic respiration was a major component of our observed soil efflux interaction over time, given certain assumptions and caveats (43, 44). Root respiration is driven by a number of factors, including current soil temperature, prior soil temperature (which could drive acclimation), tissue N concentration, and soil water (45-48), as well as root biomass (43). Several of these factors (e.g., soil temperature, soil moisture, and root N concentration) showed no significant difference between eCO_2 and aCO_2 plots at both low and high N

supply (*SI Appendix*, Table S5). Hence, although translating root biomass into absolute values of simulated soil respiration is challenging, assuming that root biomass is a reliable measure of relative differences in autotrophic respiration seems sound.

To evaluate whether root biomass mirrored the shifting N effect on eCO_2 stimulation of soil respiration, we examined its responses to CO_2 and N. In Phase I, eCO_2 stimulated root biomass to similar extents at low (11%) and high N (14%) supply (*SI Appendix*, Fig. S1e), which might partially account for the parallel responses of soil respiration to eCO_2 at low and high N supply (Fig. 1b). In contrast, live root biomass was stimulated more by eCO_2 at high N (22%) than low N (14%) supply in Phase II (*SI Appendix*, Fig. S1f), whereas soil respiration was stimulated less by eCO_2 at high N (19%) than at low N (40%) supply (Fig. 1c). Thus, live root biomass and associated autotrophic respiration responses likely were not the main drivers of the shifting responses of soil respiration to CO_2 and N treatments, as mentioned above (*SI Appendix*, Table S4).

To examine the potential importance of different microbial processes in explaining the phase shift in CO_2×N interactive effects on soil respiration, we analyzed the composition and abundance of microbial functional genes for soil samples collected in 2009 using GeoChip (49). GeoChip is a generic microarray targeting hundreds of functional gene categories important to biogeochemical, ecological, and bioremediation processes. As predicted, the functional community structure was significantly shifted by CO_2, N, and plant diversity treatments (*SI Appendix*, Table S6). All functional gene categories involved in C degradation and N cycling showed significant ($p \leq 0.05$) or marginally significant ($p \leq 0.10$) correlations across plots with mean soil CO_2 efflux in Phase II (*SI Appendix*, Table S7), but none of them did so in Phase I ($p > 0.10$). Thus,

271 microbial communities could play an important role in mediating the phase shift of N-
272 induced differences in the soil respiration response to eCO_2.

273 Directly relevant to questions of CO_2×N interactive effects on soil CO_2 efflux in
274 Phase II, many microbial genes involved in C degradation and N cycling were
275 significantly stimulated or suppressed by eCO_2, but in different ways at low than at high
276 N supply (Fig. 2). In general, at low N supply, most genes related to C degradation and N
277 cycling were stimulated by eCO_2 (Fig. 2a), whereas at high N supply, most were slightly
278 suppressed (Fig. 2b). Among those genes, antagonistic CO_2×N effects, whereby the
279 combined CO_2 and N effect on functional gene abundance was less than additive, were
280 dominant (67%) (*SI Appendix*, Table S8), but no synergistic interactive effects were
281 observed (50). Additionally, to summarize gene responses across all 14 assessed gene
282 categories (in addition to those in Fig. 2a and Fig. 2b), we determined the percentage of
283 the significantly shifted genes (for each function) that increased versus decreased at eCO_2,
284 at each of the two N supply rates. A markedly greater percentage (59%) of affected genes
285 were stimulated by eCO_2 at low than at high N supply (Fig. 2c vs. Fig. 2d; $p = 0.04$ for
286 CO_2×N effect on the relative abundance of those genes, *SI Appendix*, Table S6).
287 Altogether, the changes in various functional gene abundances suggest enhanced
288 microbial decomposition response to eCO_2 at low N supply. These results are consistent
289 with the above experimental observations that the effects of eCO_2 on soil respiration in
290 Phase II were more enhanced at low N than at high N supply.

291 In parallel with changes in overall community functions, CO_2 and N showed
292 antagonistically interactive effects on a variety of bacterial genes (26% of the bacterial
293 genes on the arrays) related to C degradation and N cycling, which were significantly (*p*

294 < 0.05) stimulated by eCO_2 at low N supply but were suppressed by eCO_2 at high N
295 supply (*SI Appendix,* Table S9). However, only three fungal genes (15%) related to C
296 degradation were antagonistically affected by CO_2 and N, while most of the fungal genes
297 (85%) showed similar responses to eCO_2 at the two N supplies. The results suggest that
298 high N supply suppressed the eCO_2 effect on bacterial functional capacity, thus
299 potentially shifting the microbial community toward relatively higher fungal capacity.
300 Two major competing, but non-exclusive, theories have been proposed to explain
301 the mechanisms underlying the impacts of N on eCO_2-induced microbial decomposition
302 of SOM (23). Herein, we identify which ones may be at work in BioCON. The
303 "stoichiometric decomposition" theory posits that microbial activity (e.g., decomposition,
304 respiration) will be highest when the stoichiometry of substrates matches that of
305 microbial demand and C and N co-limit decomposition (51). Accordingly, soil respiration
306 will be stimulated more by eCO_2 at high than at low N supply (*SI Appendix,* Table S10).
307 This is because with higher substrate C/N ratios at eCO_2 and low N supply, microbes are
308 unable to meet their N demand, which may suppress microbial C decomposition rates and
309 disfavor rapidly growing microbes (r-strategists) that primarily use labile C. In contrast,
310 the "microbial N mining" theory asserts that, at low N availability, microbes use labile C
311 as an energy source to decompose recalcitrant SOM to acquire N, accelerating microbial
312 decomposition of SOM and favoring genes involved in recalcitrant C degradation (slow-
313 growing k-strategists) (*SI Appendix,* Table S10) (52).
314 Data from BioCON in Phase II are more consistent with the microbial N limitation
315 and N mining theory. eCO_2 significantly increased soil net N mineralization at high, but
316 not low, N supply (*SI Appendix,* Fig. S1b) and the aboveground plant N concentration

and total plant N pool were considerably less under low than high N supply (*SI Appendix*, Fig. S1d, h). Those results suggest limited N availability at low N supply may not have met microbial N demand, and hence microbial C decomposition was stimulated to acquire N. As a likely result, most genes involved in C and N cycling were stimulated by eCO_2 at low N supply (Fig. 2a), in contrast to their suppression by eCO_2 at high N supply (Fig. 2b). Alternatively, eCO_2 weakly ($p = 0.08$) decreased soil C/N ratio at low but not high N supply (*SI Appendix*, Fig. S1j). As microbial C content relative to N is one to two orders of magnitude lower than that of plants (51), a decreased soil substrate C/N ratio may relieve nutrient limitation and promote substrate-induced microbial respiration (53), echoing the stoichiometric decomposition theory. It should be noted that N addition could reduce soil respiration (12-15) by suppressing microbial decomposition via both N-mining and substrate stoichiometry, which are time-dependent and may take a long time to appear. This could be one of the main reasons that the N-induced suppression of the stimulatory effects of eCO_2 on soil respiration was more obvious in Phase II.

Decomposition modeling enabled by microbial functional traits

As demonstrated above, microbial functional community structure likely plays an important role in mediating responses of soil respiration to eCO_2 and N availability. Such information is a prerequisite for predicting how the soil microbial community and associated functions respond to multiple global change factors. The next urgent need is to translate such conceptual understanding into an ecosystem model-based quantitative framework because process-based microbial-explicit ecosystem models can provide mechanistic insights, integration, and scenario testing not available from or possible with

340 experiments (54). In this regard, microbial-explicit ecosystem models will enable us to
341 mechanistically simulate large-scale experiments that would be too costly to establish in
342 reality and predict their future dynamics. However, a grand challenge in ecology is how
343 to integrate microbial functional traits into ecosystem models to improve their
344 performance and predictive ability (55).

345 To address the above challenge, we incorporated the GeoChip-detected microbial
346 functional genes into the C-N coupled Microbial-ENzyme Decomposition (MEND)
347 model (*SI Appendix*, Fig. S2a, and Table S11-15). We used tMEND to denote the MEND
348 model parameterized with traditional observations such as soil CO_2 efflux and mineral N
349 concentrations. For comparison, gMEND refers to the MEND model calibrated with
350 additional GeoChip-based microbial functional gene abundance data (Fig. 3a and *SI*
351 *Appendix*, Fig. S3a). We compared the results of these two microbial models (tMEND,
352 gMEND) plus a third model, the non-microbial C-only TECO model (*SI Appendix*, Fig.
353 S2b). In addition to the best fit between observed and simulated soil CO_2 efflux and
354 mineral N (NH_4^+ and NO_3^-) concentrations, we constrained the model by achieving the
355 highest goodness-of-fit between MEND-modeled relative changes in enzyme
356 concentrations and GeoChip-detected relative changes in oxidative and hydrolytic gene
357 abundances in response to eCO_2 (*SI Appendix*, Table S11).

358 The eCO_2-induced changes in hydrolytic and oxidative genes observed by GeoChip
359 were consistent with changes simulated by gMEND but not tMEND (Fig. 3a). Also, the
360 parameter uncertainty (i.e., coefficient of variation) of gMEND was considerably reduced
361 compared to both tMEND (by 35%) and the non-microbial C-only TECO model (by 86%;
362 Fig. 3b). As a result, the gMEND model was able to simulate the observed soil CO_2

efflux at aCO_2-aN relatively well (R^2 = 0.61; Fig. 3c). In addition, the gMEND model that had been calibrated only with the data at aCO_2-aN was further validated against independent datasets from the other three CO_2 and N treatments. The performance was almost as good as model calibration for ambient conditions (5% less variance explained on average) (R^2 = 0.53–0.59; Fig. 3d). In contrast, the TECO model explained considerably less variation in observed soil respiration at the other three treatment combinations (R^2 = 0.35–0.44; Fig. 3d) than at ambient conditions (explaining about 16% less of the variance). These differences suggest that gMEND better adjusts for CO_2 and N effects than TECO. Finally, gMEND-simulated ammonium and nitrate concentrations also agreed fairly well with the observations (*SI Appendix*, Fig. S3b). Altogether, the above results suggested that the gMEND model can capture the dynamics of soil CO_2 efflux reasonably well, comparable to or better than several previously field modeling studies (56, 57).

We further estimated eCO_2-induced soil C loss via heterotrophic respiration. Our simulations showed that eCO_2 would cause 38% and 20% more heterotrophic respiration at low and high N supply (Fig. 3e), respectively, and that enriched N would lead to 18% and 2% more heterotrophic respiration at aCO_2 and eCO_2 (Fig. 3e), respectively. We then asked what the implications might be if such results were general for grasslands globally. Applying our results to the world's grasslands based on the IGBP (International Geosphere-Biosphere Programme) classification scheme and the estimated annual soil respiration from grasslands between 2001 and 2009 (58), eCO_2 (+180 ppm) alone would increase heterotrophic respiration by 1.6 ± 0.1 Pg C yr^{-1} whereas enriched N (+4 g N m^{-2} yr^{-1}) alone would increase heterotrophic respiration by 0.8 ± 0.2 Pg C yr^{-1} However,

386 combined eCO_2 and enriched N would increase heterotrophic respiration by 1.7 ± 0.2 Pg
387 C yr^{-1} across global grasslands, 29% less than the additive effects of eCO_2 and enriched
388 N alone. Thus, interactions noted herein could be significant globally.

389 Although our modeling results via calibration (Fig. 3a-c) and validation (Fig. 3d)
390 indicated that the gMEND could encapsulate the dynamics of soil CO_2 efflux fairly well,
391 about 40% of the variation was not captured, likely for two primary reasons. First,
392 various experimental measurements such as gross primary productivity, soil CO_2 efflux,
393 temperature, moisture, and microbial traits were highly variable and some were uncertain,
394 which could contribute to the discrepancy between model simulations and experimental
395 observations. Second, the MEND model used in this study does not consider the
396 differential roles of diverse microbial communities (e.g., bacteria, saprotrophic and
397 mycorrhizal fungi) in regulating C-N cycling in response to eCO_2 and enriched N supply
398 owing to our poor understanding of these processes (8). Incorporating additional
399 biological processes and their interactions into the MEND model may improve the
400 modeling of soil CO_2 efflux and its response to environmental change (8). Nevertheless,
401 to our knowledge, this is the first demonstration of the feasibility of integrating massive
402 omics information into ecosystem models for better predictions of the soil C response to
403 eCO_2 and enriched N.

404

405 **Conclusions**

406 We found that the positive effect of eCO_2 on soil respiration at low N supply was greater
407 in years 9-12 than in years 1-8 of a long-term experiment, and that changes in microbial
408 functional traits, such as functional genes involved in C and N cycling processes, as well

as temporal shifts in soil and plant N availability, likely underlie this dynamic. These findings would, if general, have important implications for predicting the responses of ecosystems to future environmental changes. For example, considering that N limitation is widespread in natural ecosystems, considerable stimulation of soil respiration in response to rising CO_2 concentration might occur. Pervasive N deposition due to anthropogenic activities could offset, at least partially, the stimulation of soil respiration by elevated atmospheric CO_2, and thus could weaken the positive feedback between the terrestrial C cycle and climate change. Our study also shows that whether microbially mediated feedback to rising CO_2 concentrations and climate change is positive or negative depends on microbial functional groups and whether their associated functions are stimulated by eCO_2, suggesting the necessity of integrating microbial functional traits into climate-C models for better prediction (34, 55). As expected, incorporating those functional genes into a coupled C-N ecosystem model substantially reduced model parameter uncertainty and improved the prediction of soil respiration in response to eCO_2 and enriched N supply. Although further model development, calibration, and validation of a microbially-enabled model will require rigorous benchmarking with observations, this study serves as a novel step forward to mechanistically assimilate microbial functional traits into climate-C cycle modeling.

Materials and methods

Experimental design and sampling

The BioCON experiment contains 296 main plots with a fully factorial 2×2×4 combinations of three treatments: CO_2 (ambient vs. +180 ppm), N deposition (ambient vs.

+4 g N m^{-2} y^{-1}) and plant diversity (1, 4, 9 or 16 species) (59). Plots were established with diversity treatments in 1997. The CO_2 and N treatments began in 1998. The 296 plots are evenly distributed among six rings with split-plot arrangement of CO_2 and N treatments. CO_2 treatment is the whole-plot factor. The subplot N and plant diversity treatments were randomly distributed and replicated in individual plots among the six rings. Although ambient CO_2 concentration has increased during the experimental period, resulting in inconstant ambient CO_2 concentrations over time, a free-air CO_2 enrichment system is used to provide a constant elevation of CO_2 by an average of 180 ppm above ambient in three elevated CO_2 (eCO_2) rings. The other three ambient CO_2 rings (aCO_2) were treated identically but without additional CO_2. Half of the plots in each ring received N amendments of 4 g N m^{-2} yr^{-1} applied as NH_4NO_3 on three dates each year. As a consequence, there were in total four CO_2 and N treatments among 296 plots: aCO_2 & low N (aCO_2-aN), eCO_2 & low N (eCO_2-aN), aCO_2 & high N (aCO_2-eN), and eCO_2 & high N (eCO_2-eN) with each treatment having 74 plots (biological replicates). For each of the four CO_2 and N treatments, there were 32 plots planted with 1 species, 15 plots planted with 4 species, 15 plots planted with 9 species, and 12 plots planted with 16 species (59).

Plant and soil variables

Each year (1998–2009) in every plot, above- and below-ground (0-20 cm depth) plant biomass were mainly measured in August (59). Soil net N mineralization rates were measured *in situ* each year in each plot for a ca. 1-month period using a semi-open core in July (24). Net N mineralization is the net transformation of N from organic to inorganic

forms and is considered to represent the availability of N to plants. Plant N concentration (% aboveground plant and root) and plant C/N ratio (aboveground plant and root) were measured in August from 2001 to 2009. Soil C/N ratio was measured in year 2002 and 2007.

Soil CO_2 efflux in each plot was measured for 11 to 36 times per year using an LI-COR 6400-09 soil CO_2 efflux chamber (LI-COR, Lincoln, Nebraska, USA) from 1998 to 2009. Measurements made during peaking growing seasons (from May to August) were used in this study, as those data best reflect growing season ecosystem functioning. Within each of those months, soil CO_2 efflux was measured 2 to 5 times in each plot. In the short term, soil CO_2 efflux measured using chamber techniques may deviate from the instantaneous soil respiration due to changing CO_2 stored in the soil pore-space (60). However, in the medium to long term, soil CO_2 efflux corresponds to soil respiration as all CO_2 produced in the soil must be emitted from the soil. Thus, in this study, we use "soil CO_2 efflux" and "soil respiration" in an exchangeable way.

GeoChip experiments and raw data processing

Soil samples for microbial community analysis were collected from the 296 plots in August 2009. Microbial genomic DNA was extracted from 5 g of well-mixed soil for each sample by combining freeze-grinding and sodium dodecyl sulfate for cell lysis, and purified by agarose gel electrophoresis, followed by phenol–chloroform–butanol extraction as previously described (61). The functional gene array GeoChip 4.0 was used for DNA microarray hybridization. As described previously (62), the DNA samples were labeled with fluorescent dye Cy-3 dUTP and hybridized with the slides with GeoChip

4.0M in a rotator/incubator at 67 ^{o}C plus 10% formamide and rotated at 20 rpm for 24 hours. After hybridization, GeoChip was scanned at 100% laser power and 100% photomultiplier tubes gain with a NimbleGen MS 200 Microarray Scanner (Roche NimbleGen, Madison, WI, USA). Scanned images were gridded by NimbleScan software (Roche, South San Francisco, CA, USA) to obtain the signal intensity for each probe. Raw data obtained from NimbleScan was submitted to the Microarray Data Manager at http://ieg.ou.edu/microarray/ and analyzed by the data analysis pipeline (49). We removed spots with the signal-to-noise ratio below 2, considered as poor quality.

Model simulation and prediction

Details for modeling methods are provided in *SI Appendix*, Supplementary Text. Briefly, we used a non-microbial C-only terrestrial ecosystem (TECO) model and a C-N coupled Microbial-ENzyme Decomposition (MEND) model to simulate daily soil CO_2 efflux for four CO_2 and N treatments from 1998 to 2009. In TECO model, we used a group of first-order ordinary differential equations (ODEs) to describe the C turnover among fast, slow, and passive SOM pools (*SI Appendix*, Fig. S2b). We set prior ranges of C turnover rates based on a previous study (63), which were modified by soil temperature (*T*) and moisture (*W*) during the simulations. In comparison, The C-N coupled MEND model describes both C and N transformation processes in the following pools: oxidative and hydrolytic particulate organic matter (POM_O and POM_H), mineral-associated organic matter (MOM), active MOM (QOM), dissolved organic matter (DOM), active and dormant microbial biomass (MB_A and MB_D), three enzyme functional groups, and mineral N (NH_4^+ and NO_3^-) (*SI Appendix*, Fig. S2a). The two POM pools are

501 decomposed by oxidative or hydrolytic enzymes, while the MOM is decomposed by both.
502 Model state variables, governing equations, component fluxes, and parameters are shown
503 in *SI Appendix*, Table S12–S15.

504 The modified Shuffled Complex Evolution (SCE) algorithm was used to calibrate
505 model parameters for both TECO and MEND models under the aCO_2-aN treatment (*SI*
506 *Appendix*, Supplementary Text). We then validated the model using the same set of
507 model parameters calibrated for aCO_2-aN to simulate soil CO_2 efflux under the other
508 three treatments. Microbial gene abundances were used as objective functions to calibrate
509 model parameters only for the gMEND model (57). The coefficient of determination (R^2)
510 was used to estimate the model performance between simulated and observed soil CO_2
511 efflux (64). Additional observational variables (NH_4^+ and NO_3^- concentrations, response
512 ratios of oxidative and hydrolytic enzymes) for MEND model calibration and validation
513 are shown in *SI Appendix*, Table S11. Parameter uncertainty of TECO model was
514 quantified by probabilistic inversion (Markov Chain Monte Carlo) algorithm while that
515 of MEND model was quantified by the Critical Objective Function Index (COFI) method.
516

517 **Statistical analyses**

518 Since microbial community structure was determined with all 296 soil samples collected
519 in 2009, this study focused on the soil CO_2 efflux from the beginning of the BioCON
520 experiment until 2009. To identify the year in which interaction between CO_2 and N
521 emerged, we calculated the response ratio (RR) of soil CO_2 efflux differences between
522 eCO_2 and aCO_2 at low or high N supply in every month of the growing season. The N
523 influence was then calculated as RR at high N supply minus RR at low N supply,

524 representing the CO_2×N interaction. The annual mean value of the N influence was
525 calculated for each year. Four commonly used change-point tests, including Buishand
526 Range Test, Buishand U Test, Standard Normal Homogeneity Test (SNHT), and Pettitt's
527 test, were performed on the annual mean values of the N influence. Because no soils were
528 collected for microbial analysis in Phase I, most of the statistics-based mechanistic
529 analyses were focused on Phase II.

530 For each year from 1998 to 2009, data points of soil CO_2 efflux ($\mu mol\ mol^{-2}\ s^{-1}$) that
531 were higher than mean plus 1.96 standard deviations or lower than mean minus 1.96
532 standard deviations of all data points in a plot were regarded as outliers and removed
533 before the analysis (65). By doing this, we reduced the within-plot variation in soil CO_2
534 efflux measurements to enhance the statistic power. We used the same approach to
535 identifying and excluding outliers for other soil and plant variables, including soil net N
536 mineralization rate ($mg\ Kg^{-1}\ day^{-1}$), soil temperature (°C), soil moisture, soil pH, soil C/N
537 ratio, plant N concentration (%), plant C/N ratio, plant biomass ($g\ m^{-2}$) and plant N pool
538 ($g\ m^{-2}$). Net N mineralization data in 2008 were contaminated and thus were not included
539 in the analysis (41). The significance of CO_2×N effects and CO2×N×Phase effects on soil
540 CO2 efflux, soil, and plant variables was tested using repeated-measures mixed models
541 following the previous method (66). The CO_2×N effects (N influence on the eCO_2 effect)
542 on each of the soil and plant variables, and on soil CO_2 efflux were calculated per year
543 from 1998 to 2009, then relationships between CO_2×N effects on soil/plant variables and
544 on soil CO_2 efflux were examined using Pearson correlation.

The eCO_2 effects on soil and plant variables as well as microbial functional genes at low and high N supply were calculated based on Eq. 3-4:

$$eCO_2 \text{ effect at low N supply} = 100\% \times \frac{\overline{eCaN} - \overline{aCaN}}{\overline{aCaN}} \quad (3)$$

$$eCO_2 \text{ effect at high N supply} = 100\% \times \frac{\overline{eCeN} - \overline{aCeN}}{\overline{aCeN}} \quad (4)$$

Where $\overline{eCeN}$, $\overline{eCaN}$, $\overline{aCeN}$ and $\overline{aCaN}$ represent mean of soil CO_2 efflux, soil variables, plant variables, or the relative abundance of microbial functional genes in eCO_2-eN, eCO_2-aN, aCO_2-eN, and aCO_2-aN plots, respectively. Permutation *t*-test was conducted to examine the significance of the eCO_2 effect on plant and soil properties at both low and high N supply (67). At the low or high N supply, the significance of eCO_2 effect on the abundance of each functional gene (total abundance of all probes of this gene; ***SI Appendix***, Table S8) was examined by response ratio with 95% confidence intervals of gene abundance differences between eCO_2 and aCO_2 plots. We also examined the eCO_2 effect on the abundance of each gene probe by response ratio. Of all significantly changed probes of an individual gene, we calculated the percentages of stimulated and suppressed probes by eCO_2. Then, we calculated the averaged percentages of stimulated and suppressed probes across genes in different gene categories for C cycling, including starch, hemicellulose, cellulose, chitin, pectin, aromatics and lignin degradation, gene categories for N cycling, including assimilatory/dissimilatory N reduction, denitrification, ammonification, nitrification and N fixation as well as gene categories for phosphorus (P) cycling, including P fixation and P utilization.

To determine the direction (additive, synergistic, or antagonistic) of interactive effects of CO_2 and N on functional genes, we compared the observed effects (OEs, i.e., combined eCO_2 and enriched N effects) and the expected effects (EEs), i.e., additive

effects of eCO_2 alone and enriched N alone (50). For each functional gene, OE was calculated as follows: $100\% \times \frac{\overline{eCeN} - \overline{aCaN}}{\overline{aCaN}}$. EE was calculated as follows: $100\% \times \frac{\overline{eCaN} - \overline{aCaN}}{\overline{aCaN}} + 100\% \times \frac{\overline{aCeN} - \overline{aCaN}}{\overline{aCaN}}$. The interactive effects are additive when OE is not different from EE. Interactive effects are synergistic if OE is significantly higher than EE or antagonistic if OE is significantly lower than EE. The significance of the interactive CO_2 and N effect on each functional gene was tested by the permutational multivariate analysis of variance (Adonis) using the abundance matrix of this microbial functional gene.

Acknowledgments

The data analysis by Qun Gao was supported by the National Science Foundation of China (41825016) and the Second Tibetan Plateau Scientific Expedition and Research (STEP) program (2019QZKK0503) to Yunfeng Yang. The BioCON experiment was funded by the United States Department of Agriculture (Project 2007-35319-18305) through NSF-USDA Microbial Observatories Program, the U.S. National Science Foundation (NSF) Long-Term Ecological Research (DEB-0620652, DEB-1234162), Long-Term Research in Environmental Biology (DEB-1242531), and Ecosystem Sciences (NSF DEB-1120064) Programs; as well as the U.S. Department of Energy Program for Ecosystem Research (DE-FG02-96ER62291) to Peter Reich and/or Sarah Hobbie. The experimental measurements with GeoChip were supported by the United States Department of Agriculture (Project 2007-35319-18305) through the NSF-USDA Microbial Observatories Program, and the modeling work was supported by the U.S. Department of Energy, Office of Science, Genomic Science Program under Award

591 Numbers DE-SC0004601, DE-SC0010715, DE-SC0014079, DE-SC0016247, and DE-
592 SC0020163 and by the Office of the Vice President for Research at the University of
593 Oklahoma, all to Jizhong Zhou.
594

595 **Competing interest**

596 The authors declare no competing interest.
597

References

1. A. Arneth *et al.*, Terrestrial biogeochemical feedbacks in the climate system. *Nature Geoscience* **3**, 525-532 (2010).
2. C. Oertel, J. Matschullat, K. Zurba, F. Zimmermann, S. Erasmi, Greenhouse gas emissions from soils—A review. *Geochemistry* **76**, 327-352 (2016).
3. T. D. Lee, S. H. Barrott, P. B. Reich, Photosynthetic responses of 13 grassland species across 11 years of free-air CO2 enrichment is modest, consistent and independent of N supply. *Global Change Biology* **17**, 2893-2904 (2011).
4. R. Matamala, H. Schlesinger William, Effects of elevated atmospheric CO2 on fine root production and activity in an intact temperate forest ecosystem. *Global Change Biology* **6**, 967-979 (2001).
5. A. E. Carol, P. B. Reich, J. J. Trost, S. E. Hobbie, Elevated CO2 stimulates grassland soil respiration by increasing carbon inputs rather than by enhancing soil moisture. *Global Change Biology* **17**, 3546-3563 (2011).
6. S. Liu *et al.*, Climatic role of terrestrial ecosystem under elevated CO2: a bottom‐up greenhouse gases budget. *Ecology Letters* **21**, 1108-1118 (2018).
7. J. Heath *et al.*, Rising atmospheric CO2 reduces sequestration of root-derived soil carbon. *Science* **309**, 1711-1713 (2005).
8. M. A. Bradford *et al.*, Managing uncertainty in soil carbon feedbacks to climate change. *Nature Climate Change* **6**, 751-758 (2016).
9. Y. Li *et al.*, Increasing importance of deposition of reduced nitrogen in the United States. *Proceedings of the National Academy of Sciences* **113**, 5874-5879 (2016).
10. L. Zhou *et al.*, Different responses of soil respiration and its components to nitrogen addition among biomes: a meta-analysis. *Global Change Biology* **20**, 2332-2343 (2014).
11. Z. Chen *et al.*, Extreme rainfall and snowfall alter responses of soil respiration to nitrogen fertilization: a 3-year field experiment. *Global Change Biology* **23**, 3403-3417 (2017).
12. I. A. Janssens *et al.*, Reduction of forest soil respiration in response to nitrogen deposition. *Nature Geoscience* **3**, 315-322 (2010).
13. P. Olsson, S. Linder, R. Giesler, P. Högberg, Fertilization of boreal forest reduces both autotrophic and heterotrophic soil respiration. *Global Change Biology* **11**, 1745-1753 (2005).
14. D. Ward, K. Kirkman, N. Hagenah, Z. Tsvuura, Soil respiration declines with increasing nitrogen fertilization and is not related to productivity in long-term grassland experiments. *Soil Biology and Biochemistry* **115**, 415-422 (2017).
15. Z. Sun *et al.*, The effect of nitrogen addition on soil respiration from a nitrogen-limited forest soil. *Agr Forest Meteorol* **197**, 103-110 (2014).
16. Q. Peng *et al.*, Effects of nitrogen fertilization on soil respiration in temperate grassland in Inner Mongolia, China. *Environmental Earth Sciences* **62**, 1163-1171 (2011).
17. Y. Qi, Differential responses of short-term soil respiration dynamics to the experimental addition of nitrogen and water in the temperate semi-arid steppe of Inner Mongolia, China. *Journal of Environmental Sciences* **26**, 834-845 (2014).
18. T. F. Stocker, D. Qin, G.-K. Plattner, M. M. B. Tignor, IPCC, 2013: Climate change 2013: The physical science basis. Contribution of working group I to the fifth assessment report of the Intergovernmental Panel on Climate (Cambridge University Press, Cambridge, United Kingdom and New York, NY, USA, 2013), pp.1535.

19. Q. Deng *et al.*, Responses of soil respiration to elevated carbon dioxide and nitrogen addition in young subtropical forest ecosystems in China. *Biogeosciences* **7**, 315-328 (2010).
20. Q. Deng *et al.*, Seasonal responses of soil respiration to elevated CO2 and N addition in young subtropical forest ecosystems in southern China. *Ecological Engineering* **61**, 65-73 (2013).
21. M. Craine Joseph, A. Wedin David, B. Reich Peter, The response of soil CO2 flux to changes in atmospheric CO2, nitrogen supply and plant diversity. *Global Change Biology* **7**, 947-953 (2001).
22. J. M. Melillo *et al.*, Soil warming, carbon–nitrogen interactions, and forest carbon budgets. *Proceedings of the National Academy of Sciences* **108**, 9508-9512 (2011).
23. R. Chen *et al.*, Soil C and N availability determine the priming effect: microbial N mining and stoichiometric decomposition theories. *Global Change Biology* **20**, 2356-2367 (2013).
24. P. B. Reich *et al.*, Nitrogen limitation constrains sustainability of ecosystem response to CO2. *Nature* **440**, 922-925 (2006).
25. S. Fontaine *et al.*, Stability of organic carbon in deep soil layers controlled by fresh carbon supply. *Nature* **450**, 277-280 (2007).
26. E. C. Adair, P. B. Reich, S. E. Hobbie, J. M. Knops, Interactive effects of time, CO2, N, and diversity on total belowground carbon allocation and ecosystem carbon storage in a grassland community. *Ecosystems* **12**, 1037-1052 (2009).
27. C. M. Litton, J. W. Raich, M. G. Ryan, Carbon allocation in forest ecosystems. *Global Change Biology* **13**, 2089-2109 (2007).
28. W. Cheng *et al.*, Synthesis and modeling perspectives of rhizosphere priming. *New Phytologist* **201**, 31-44 (2013).
29. F. Dijkstra, Y. Carrillo, E. Pendall, J. Morgan, Rhizosphere priming: a nutrient perspective. *Frontiers in Microbiology* **4**, 00216 (2013).
30. M. Carreiro, R. Sinsabaugh, D. Repert, D. Parkhurst, Microbial enzyme shifts explain litter decay responses to simulated nitrogen deposition. *Ecology* **81**, 2359-2365 (2000).
31. B. Wild *et al.*, Input of easily available organic C and N stimulates microbial decomposition of soil organic matter in arctic permafrost soil. *Soil Biology and Biochemistry* **75**, 143-151 (2014).
32. R. Cavicchioli *et al.*, Scientists' warning to humanity: microorganisms and climate change. *Nature Reviews Microbiology* **17**, 569-586 (2019).
33. T. Crowther *et al.*, The global soil community and its influence on biogeochemistry. *Science* **365**, eaav0550 (2019).
34. J. Zhou *et al.*, Microbial mediation of carbon-cycle feedbacks to climate warming. *Nature Climate Change* **2**, 106-110 (2011).
35. X. Guo *et al.*, Gene-informed decomposition model predicts lower soil carbon loss due to persistent microbial adaptation to warming. *Nature Communications* **11**, 4897 (2020).
36. F. A. Dijkstra, S. E. Hobbie, P. B. Reich, J. M. H. Knops, Divergent effects of elevated CO2, N fertilization, and plant diversity on soil C and N dynamics in a grassland field experiment. *Plant and Soil* **272**, 41-52 (2005).
37. P. B. Reich *et al.*, Do species and functional groups differ in acquisition and use of C, N and water under varying atmospheric CO2 and N availability regimes? A field test with 16 grassland species. *New Phytologist* **150**, 435-448 (2001).
38. D. R. Zak, W. E. Holmes, A. C. Finzi, R. J. Norby, W. H. Schlesinger, SOIL NITROGEN CYCLING UNDER ELEVATED CO2: A SYNTHESIS OF FOREST FACE EXPERIMENTS. *Ecological Applications* **13**, 1508-1514 (2003).

39. J. M. Melillo *et al.*, Long-term pattern and magnitude of soil carbon feedback to the climate system in a warming world. *Science* **358**, 101-105 (2017).
40. J. Melillo *et al.*, Soil warming and carbon-cycle feedbacks to the climate system. *Science* **298**, 2173-2176 (2002).
41. P. B. Reich, S. E. Hobbie, Decade-long soil nitrogen constraint on the CO2 fertilization of plant biomass. *Nature Climate Change* **3**, 278-282 (2013).
42. X. Zhou *et al.*, Concurrent and lagged impacts of an anomalously warm year on autotrophic and heterotrophic components of soil respiration: a deconvolution analysis. *New Phytologist* **187**, 184-198 (2010).
43. X. Wang, B. Zhu, Y. Wang, X. Zheng, Field measures of the contribution of root respiration to soil respiration in an alder and cypress mixed plantation by two methods: trenching method and root biomass regression method. *European Journal of Forest Research* **127**, 285 (2008).
44. Y. Kuzyakov, A. A. Larionova, Root and rhizomicrobial respiration: A review of approaches to estimate respiration by autotrophic and heterotrophic organisms in soil. *Journal of Plant Nutrition and Soil Science* **168**, 503-520 (2005).
45. O. K. Atkin, D. Bruhn, V. M. Hurry, M. G. Tjoelker, Evans Review No. 2: The hot and the cold: unravelling the variable response of plant respiration to temperature. *Functional Plant Biology* **32**, 87-105 (2005).
46. P. B. Reich, M. B. Walters, M. G. Tjoelker, D. Vanderklein, C. Buschena, Photosynthesis and respiration rates depend on leaf and root morphology and nitrogen concentration in nine boreal tree species differing in relative growth rate. *Functional Ecology* **12**, 395-405 (1998).
47. J. M. Craine, D. A. Wedin, F. S. Chapin, P. B. Reich, Relationship between the structure of root systems and resource use for 11 North American grassland plants. *Plant Ecology* **165**, 85-100 (2003).
48. J. C. Carey *et al.*, Temperature response of soil respiration largely unaltered with experimental warming. *Proceedings of the National Academy of Sciences* **113**, 13797-13802 (2016).
49. Q. Tu *et al.*, GeoChip 4: a functional gene‐array‐based high‐throughput environmental technology for microbial community analysis. *Molecular ecology resources* **14**, 914-928 (2014).
50. K. Xue *et al.*, Annual Removal of Aboveground Plant Biomass Alters Soil Microbial Responses to Warming. *mBio* **7**, e00976 (2016).
51. D. O. Hessen, G. I. Ågren, T. R. Anderson, J. J. Elser, P. C. de Ruiter, Carbon sequestration in ecosystems: the role of stoichiometry. *Ecology* **85**, 1179-1192 (2004).
52. S. Fontaine, A. Mariotti, L. Abbadie, The priming effect of organic matter: a question of microbial competition? *Soil Biology and Biochemistry* **35**, 837-843 (2003).
53. A. S. Mamilov, O. M. Dilly, Soil microbial eco-physiology as affected by short-term variations in environmental conditions. *Soil Biology and Biochemistry* **34**, 1283-1290 (2002).
54. K. J. Locey *et al.*, Dormancy dampens the microbial distance-decay relationship. *Philosophical Transactions of the Royal Society B: Biological Sciences* **375**, 20190243 (2020).
55. K. Xue *et al.*, Tundra soil carbon is vulnerable to rapid microbial decomposition under climate warming. *Nature Climate Change* **6**, 595-600 (2016).

56. E. A. Davidson, S. Samanta, S. S. Caramori, K. Savage, The Dual Arrhenius and Michaelis–Menten kinetics model for decomposition of soil organic matter at hourly to seasonal time scales. *Global Change Biology* **18**, 371-384 (2012).
57. G. Wang *et al.*, Soil moisture drives microbial controls on carbon decomposition in two subtropical forests. *Soil Biology and Biochemistry* **130**, 185-194 (2019).
58. J. Scurlock, D. Hall, The global carbon sink: a grassland perspective. *Global Change Biology* **4**, 229-233 (1998).
59. P. B. Reich *et al.*, Plant diversity enhances ecosystem responses to elevated CO2 and nitrogen deposition. *Nature* **410**, 809 (2001).
60. M. Maier, H. Schack-Kirchner, E. E. Hildebrand, D. Schindler, Soil CO2 efflux vs. soil respiration: Implications for flux models. *Agr Forest Meteorol* **151**, 1723-1730 (2011).
61. J. Zhou, M. A. Bruns, J. M. Tiedje, DNA recovery from soils of diverse composition. *Applied and environmental microbiology* **62**, 316-322 (1996).
62. Y. Yang *et al.*, Responses of the functional structure of soil microbial community to livestock grazing in the Tibetan alpine grassland. *Global change biology* **19**, 637-648 (2013).
63. E. Weng, Y. Luo, Relative information contributions of model vs. data to short‐and long‐term forecasts of forest carbon dynamics. *Ecological Applications* **21**, 1490-1505 (2011).
64. R. Xu, Measuring explained variation in linear mixed effects models. *Statistics in Medicine* **22**, 3527-3541 (2003).
65. J. M. Bland, D. G. Altman, Statistics notes: Measurement error. *British Medical Journal* **312**, 1654 (1996).
66. E. Moser, A. Saxton, S. Pezeshki, Repeated measures analysis of variance: application to tree research. *Canadian Journal of Forest Research* **20**, 524-535 (1990).
67. G. Alberti, *'perm.t.test': R function for permutation-based t-test* (2016), 10.13140/RG.2.2.16735.46248.

Figure legends

Figure 1. Observed responses of soil CO_2 efflux to eCO_2 at different N supply levels. **a**, soil CO_2 efflux from 1998 to 2009. **b**, soil CO_2 efflux from 1998 to 2005 (Phase I). **c**, soil CO_2 efflux from 2006 to 2009 (Phase II). Each bar shows the annual mean plus standard error of 74 plots. Percent changes of soil CO_2 efflux in elevated CO_2 (eCO_2) plots relative to ambient CO_2 (aCO_2) plots are labeled above the bars. *p* values of the permutation *t*-test are labeled as * when $p < 0.05$ and ** when $p < 0.01$.

Figure 2. eCO_2 effects on microbial functional genes important to C and N cycling at low and high N supply. a, Response ratios of functional genes at low N supply; and **b**, at high N supply. Individual functional genes detected by GeoChip are shown on the x-axis. Error bars indicate 95% confidence intervals of gene abundance difference between eCO_2 and aCO_2. **c,** The percent of significantly shifted microbial gene probes stimulated (blue) versus suppressed (orange) by eCO_2 at low N supply; and **d,** at high N supply. Percentages of stimulated and suppressed gene probes were averaged across gene probes in each gene category (each point in the boxplot) relevant to C, N, and phosphorus (P) cycling. These gene categories (n = 14) include starch, hemicellulose, cellulose, chitin, pectin, aromatics and lignin degradation, N reduction, denitrification, ammonification, nitrification, N fixation, and phosphate limitation and phosphorus utilization.

Figure 3. Model simulations. a, Comparison of eCO_2-induced percent changes of hydrolytic and oxidative enzymes observed by GeoChip to the simulated effects by gMEND (gene-incorporated MEND model) and traditional MEND without gene

information (tMEND) at low N supply. The GeoChip data were obtained from the samples from 2009. **b**, Parameter uncertainty quantified by the Coefficient of Variation (CV) for the non-microbial C-only TECO, tMEND, and gMEND models; the bars show mean CV of 10 calibrated parameters represented by dots. **c**, Model calibration with the soil respiration (R_s, 1998–2009) at aCO_2-aN. **d**, Model validations were performed using R_s at eCO_2-aN, aCO_2-eN, and eCO_2-eN for gMEND and TECO. **e**, Percent changes of gMEND-simulated heterotrophic respiration (R_h) between different CO_2 and N levels. The error bars represent standard errors. *p* values of the permutation *t*-test are labeled as * when $p < 0.05$ and ** when $p < 0.01$.

800 **Table 1.** The main and interactive effects of CO_2, N, and plant diversity (PD) on soil CO_2
801 efflux measured from 1998 to 2009 based on repeated-measures mixed model across 296
802 plots. Significant ($p < 0.05$) effects are bolded.

	F	*p*
CO_2	763.33	**<0.01**
N	59.56	**<0.01**
PD	692.89	**<0.01**
Year	410.76	**<0.01**
CO_2×N	4.63	**0.03**
CO_2×PD	13.99	**0.01**
N×PD	2.34	0.12
CO_2×Year	9.02	**0.01**
N×Year	15.69	**0.01**
PD×Year	4.32	**0.03**
CO_2×N×PD	0.04	0.83
CO_2×N×Year	3.73	**0.05**
CO_2×PD×Year	3.02	0.08
N×PD×Year	0.16	0.69
CO_2×N×PD×Year	0.51	0.47

803

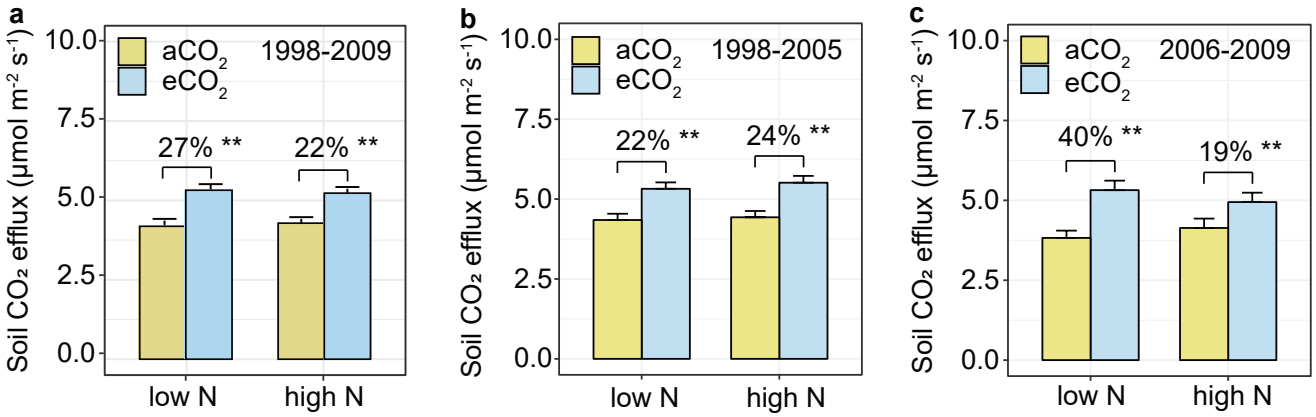
a
b
c
Soil CO₂ efflux (μmol m⁻² s⁻¹)
10.0
7.5
5.0
2.5
0.0
aCO2
eCO2
1998-2009
27% **
22% **
low N
high N
1998-2005
22% **
24% **
2006-2009
40% **
19% **

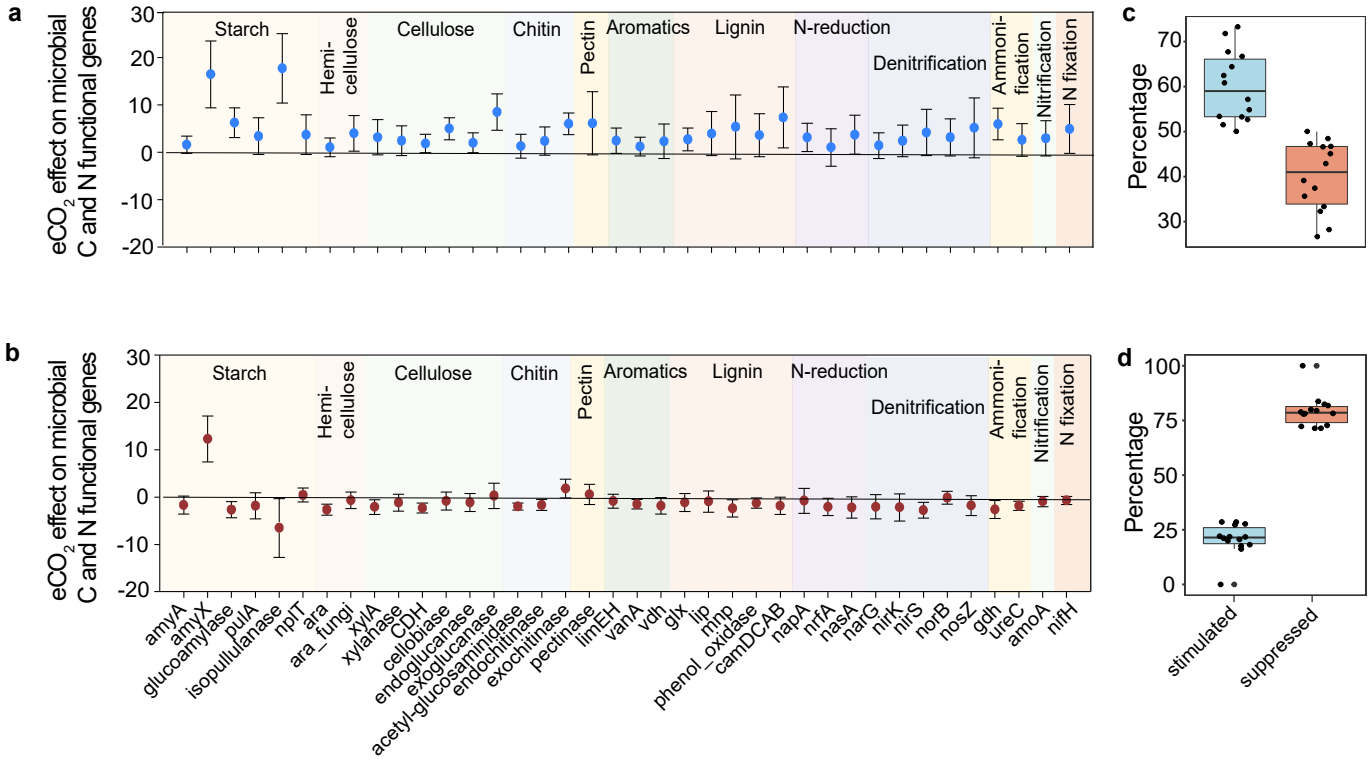
a
b
c
d
eCO2 effect on microbial C and N functional genes
Starch
Hemi-cellulose
Cellulose
Chitin
Pectin
Aromatics
Lignin
N-reduction
Denitrification
Ammoni-fication
Nitrification
N fixation
amyA
amyX
glucoamylase
pulA
isopullulanase
nplT
ara
ara_fungi
xylA
xylanase
CDH
cellobiase
endoglucanase
exoglucanase
acetyl-glucosaminidase
endochitinase
exochitinase
pectinase
limEH
vanA
vdh
glx
lip
mnp
phenol_oxidase
camDCAB
napA
nrfA
nasA
narG
nirK
nirS
norB
nosZ
gdh
ureC
amoA
nifH
Percentage
stimulated
suppressed

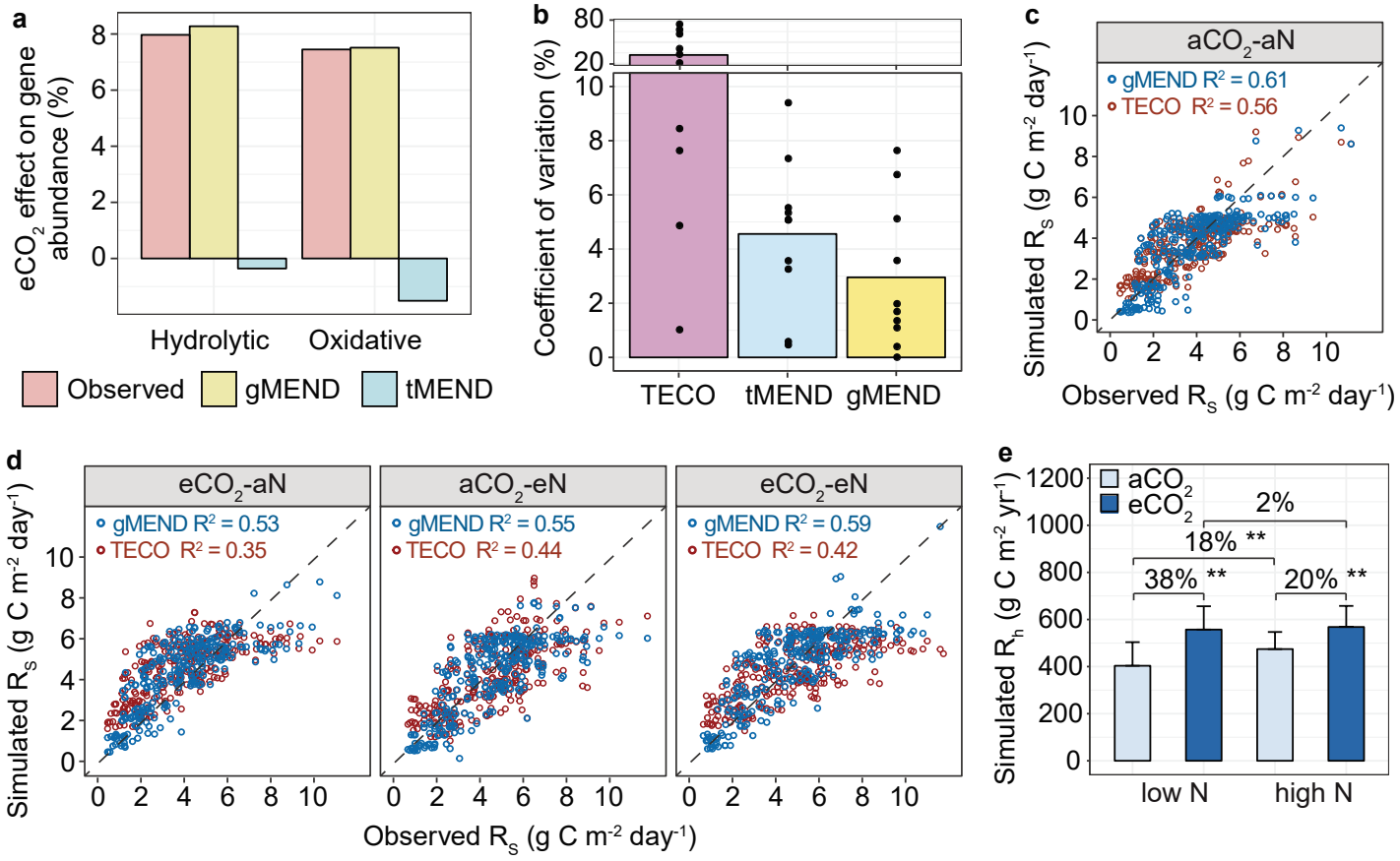
a
eCO2 effect on gene abundance (%)
Hydrolytic
Oxidative
Observed
gMEND
tMEND
b
Coefficient of variation (%)
TECO
tMEND
gMEND
c
aCO2-aN
gMEND R2 = 0.61
TECO R2 = 0.56
Simulated Rs (g C m-2 day-1)
Observed Rs (g C m-2 day-1)
d
eCO2-aN
gMEND R2 = 0.53
TECO R2 = 0.35
aCO2-eN
gMEND R2 = 0.55
TECO R2 = 0.44
eCO2-eN
gMEND R2 = 0.59
TECO R2 = 0.42
Simulated Rs (g C m-2 day-1)
Observed Rs (g C m-2 day-1)
e
aCO2
eCO2
2%
18% **
38% **
20% **
Simulated Rh (g C m-2 yr-1)
low N
high N